Proceedings of Science and Mathematics
Faculty of science, universiti teknologi malaysia
https://science.utm.my/procscimath/
Volume 8 (2025) 1-9

Targeting G6PD Deficiency: A G-Quadruplex DNA Aptamer with Enhanced Binding Towards G6PD^{Nashville} and G6PD^{Canton} Variants

Yu Suet Li[a], Nor Aina Nordin[b*], Nurriza Ab Latif[a], Syazwani Itri Amran[a*]
[a]Department of Biosciences, Faculty of Science, Universiti Teknologi Malaysia, 81310 UTM Skudai, Johor, Malaysia.
[b]Biogenes Technologies SDN BHD, Universiti Putra Malaysia, Jalan Maklumat, 43400, Serdang, Selangor, Malaysia.
*Corresponding author: aina@biogenestech.com, syazwaniitri@utm.my

Abstract
Glucose-6-phosphate dehydrogenase (G6PD) deficiency is the most common enzyme disorder caused by a genetic mutation, affecting over 500 million people worldwide. Individuals with G6PD deficiency are highly susceptible to hemolytic anemia under oxidative stress, yet current treatment is limited to blood transfusion, with no available direct therapies. Although AG1, a small-molecule G6PD activator, has shown promise, its activation effect is limited. This study presents the first G-quadruplex-forming DNA aptamers designed to target the dimer interface of two Class A G6PD mutants associated with severe hemolytic anemia (G6PD^{Nashville} and G6PD^{Canton}). Using *in silico* design via APTCAD and molecular docking, three novel aptamers (OPT1, OPT2, and OPT3) were generated and optimized for enhanced binding. Among them, OPT3 demonstrated a superior binding affinity to AG1 and targeted the overlapping binding site. Docking analysis revealed that OPT3 exhibited a stronger binding profile than AG1, forming more hydrogen bonds, electrostatic interactions, and hydrophobic contacts that promote activation and improve stabilization. These findings highlight OPT3 as a promising G6PD activator and may serve as a potential therapeutic alternative to AG1 for correcting G6PD deficiency.
Keywords: G6PD deficiency; hemolytic anemia; AG1; DNA aptamer; *in silico*

Introduction

G6PD is an enzyme that protects red blood cells (RBCs) from oxidative stress by generating reduced nicotinamide adenine dinucleotide phosphate (NADPH) through the pentose phosphate pathway. G6PD deficiency is an inherited disorder caused by mutations in the G6PD gene, leading to a shortage of NADPH and impaired antioxidant defence in RBCs. With over 400 known G6PD variants, many significantly impair enzyme activity and stability, leading to severe clinical manifestations, most notably acute hemolytic anemia (Louis et al., 2022). According to the WHO (2022), G6PD deficiency is classified into four classes (A, B, C, and U) based on enzyme activity and clinical severity.

Individuals with class A G6PD deficiency are highly susceptible to hemolytic anemia when exposed to oxidative triggers such as antimalarial drugs. Currently, blood transfusion remains the only treatment, as no direct therapies exist for G6PD deficiency. Although AG1, a small molecule G6PD activator, has shown promise, its activation effect is limited (Hwang et al., 2018; Pakparnich et al., 2021). Aptamers are short oligonucleotides that fold into stable 3D structures, enabling them to bind targets with high affinity and specificity. Several aptamers have been explored as therapeutic agents, such as aptamers developed by Tsukakoshi et al. (2021) that enhance peroxidase activity, Pegaptanib for age-related macular degeneration (Gragoudas et al., 2004) and AS1411 for targeting nucleolin in cancer therapy (Soundarajan et al., 2008).

In this study, three G-quadruplex DNA aptamers are designed *in silico* as potential G6PD activators using APTCAD. The optimization of these aptamers is guided by molecular docking targeting the dimer interface of two Class A mutants: G6PD^{Nashville} and G6PD^{Canton} that associated with severe

hemolytic anemia. Comprehensive docking analysis is also conducted to evaluate their potential as G6PD activators, and the most promising aptamer candidate is selected for *in vitro* synthesis.

Material and methods

Three natural transfer RNA (tRNA) sequences were randomly selected from GtRNAdb (https://gtrnadb.ucsc.edu/) as the templates for *in silico* aptamer design (Soon & Nordin, 2019). The selected sequences were converted to DNA by replacing uracil (U) with thymine (T) bases. The resulting DNA sequences were modified by incorporating G-rich sequences to generate G-quadruplex-forming DNA aptamers. The presence of quadruplex-forming G-rich sequences (QGRS) was validated using QGRS Mapper (https://bioinformatics.ramapo.edu/QGRS/analyze.php). The primary DNA aptamer sequences were saved in FASTA format for 2D and 3D structure prediction using APTCAD (http://www.aptcad.com/), and their folding stability values were recorded. Prior to docking, the three aptamers were set as rigid molecules by converting all rotatable bonds to non-rotatable and saved in .pdbqt file format using AutoDockTools.

The 3D structure of wild-type (WT) G6PD was prepared using crystal structures from the Protein Data Bank (2BHL and 2BH9) (Alakbaree et al., 2022; Louis et al., 2022). *In silico* site-directed mutagenesis was performed using PyMOL's Mutagenesis Wizard to generate $G6PD^{Nashville}$ (Arg393His) and $G6PD^{Canton}$ (Arg459Leu), with amino acid substitutions applied to both dimer chains. The mutant structures were saved in .pdb format and converted to .pdbqt format along with the aptamers using AutoDock Tools. The aptamers were then docked to the dimer interface of $G6PD^{Nashville}$ and $G6PD^{Canton}$ using AutoDock Vina. Docking complexes with the best binding affinities were selected and visualized in PyMOL.

Aptamer optimization was guided by visualization of the docking complexes. This allowed the identification and removal of non-interacting nucleobases that were not involved in binding at dimer interface of $G6PD^{Nashville}$ and $G6PD^{Canton}$, retaining only the core binding regions at the dimer interface. To further enhance the folding stability of the truncated aptamers, GC content was increased by substituting adenine (A) or thymine (T) bases with guanine (G) or cytosine (C) within the stem-loop regions (O'Steen & Kolpashchikov, 2022). Molecular docking was then repeated to evaluate the improvements of optimized aptamers in binding performance. Additionally, AG1, a known G6PD activator, served as the reference compound in this study. Its 3D structure was retrieved from PubChem (CID: 6615809) in .sdf format and converted to .pdb format using OpenBabel. AG1 was then docked at the dimer interface of the two G6PD mutants using AutoDock Vina.

The final molecular docking was conducted for the three optimized aptamers against $G6PD^{Nashville}$ and $G6PD^{Canton}$, evaluating binding affinities, orientations and interactions in comparison to AG1. Binding site overlap with AG1 was visualized in PyMOL, while non-covalent interactions, including hydrogen bonds, hydrophobic interactions and salt bridges, were analyzed using BIOVIA Discovery Studio and LigPlot+**.**

Results and discussion

Three G-quadruplex-forming DNA aptamers (APT1, APT2, and APT3) were designed, and their 2D structures and folding stability were predicted using APTCAD, as depicted in Figure 1. All aptamers exhibited negative folding free energy values (ΔG), indicating a thermodynamically favourable conformation. This suggests that the aptamers can bind their target efficiently without requiring external energy input (Ahmad Najib et al., 2024). Each aptamer ranged in length from 60 to 80 nucleotides and featured various stem-loop structures. The stem-loop structures were the key design element, with the stem contributing to the aptamer's structural stability, and the loop serving as a functional domain for target binding and specificity (Ji et al., 2025). The incorporation of G-rich quadruplex sequences further enhances folding stability (Roxo et al., 2019). DNA aptamers were chosen over RNA aptamers due to their greater chemical stability, as the absence of a hydroxyl group at the 2' position of the deoxyribose sugar makes them more resistant to nuclease degradation. This structural advantage also contributes to a simpler and more cost-effective synthesis process, as well as greater ease of chemical modification.

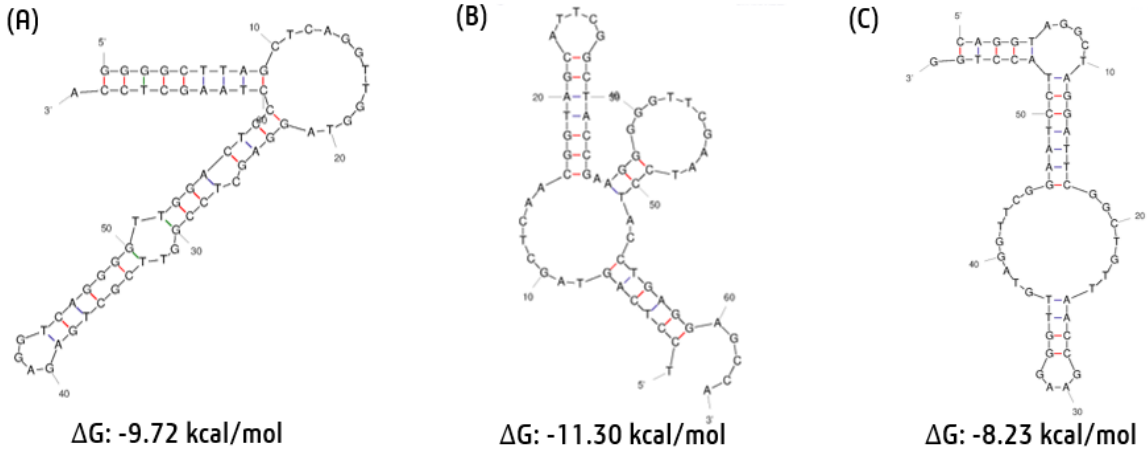

Figure 1 2D structures and folding stability values (ΔG) of designed aptamers: (A) APT1, (B) APT2, and (C) APT3.

Prior to aptamer optimization, molecular docking was used to assess the binding region of the aptamers to the dimer interface of G6PD^{Nashville} and G6PD^{Canton}. During the docking, the aptamers were treated as rigid molecules with no rotatable bonds. A rigid aptamer model is commonly used in docking studies to examine interactions with targets and assist in predicting binding affinities (Bruno, 2022). The visualization of the docked complexes with the best binding affinities was performed using PyMOL software. Since only a small portion of the full-length aptamer is typically involved in target recognition, truncating non-binding regions during the optimization process can enhance binding affinity and reduce synthesis costs by minimizing sequence length (Hui et al., 2023; Nguyen et al., 2024). Referring to Figure 2, aptamer regions consistently located distally from the dimer interface in both models were identified. Truncation was subsequently performed by removing 21 bases from APT1, 28 bases from APT2, and 20 bases from APT3.

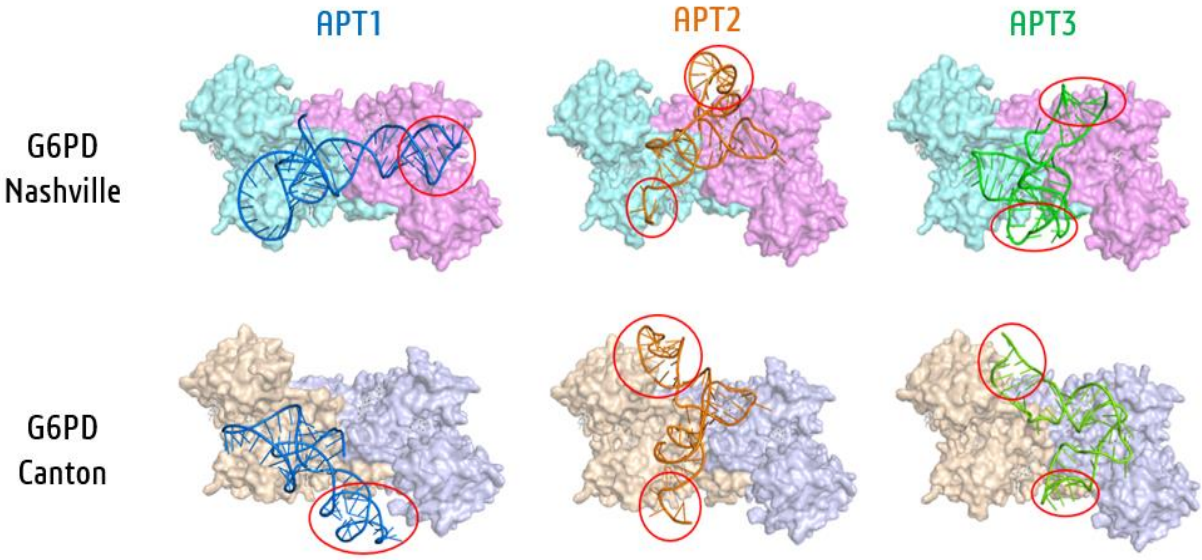

Figure 2 Docking visualizations showing the truncated regions of aptamers circled in red (APT1: blue; APT2: orange, APT3: green)

After truncating the aptamers, their folding stability was predicted again using APTCAD. However, a notable reduction in folding stability of all truncated aptamers was observed, indicated by higher ΔG values, as shown in Table 1. To address this, the GC content within the stem-loop regions

of the truncated aptamers was increased to enhance their folding stability (O'Steen & Kolpashchikov et al., 2022; Lau et al., 2025). Guanine-cytosine (GC) base pairs form three hydrogen bonds compared to two in adenine-thymine (AT) base pairs, which contributes to greater structural stability through improved core folding and higher melting temperatures. As a result, substituting nucleotides within the stem-loop regions with G and C bases led to the generation of three optimized G-quadruplex-forming DNA aptamers (OPT1, OPT2 and OPT3) with higher GC content and improved folding stability.

Table 1: Folding stability of aptamers at initial, after truncation, and after GC content modification.

Aptamer	Folding free energy values, ΔG (kcal/mol)		
	Initial	After truncation	After GC content modification
APT1	-9.72	-6.54	-8.23
APT2	-11.30	-3.29	-7.07
APT3	-8.23	-4.64	-9.61

Among the optimized aptamers, OPT3 exhibited the most stable folding structure, indicated by the lowest folding free energy (ΔG) value of −9.61 kcal/mol, followed by OPT1 and OPT2 with values of -8.23 and -7.07 kcal/mol respectively, as depicted in Figure 3. This is likely attributed to the longer stem lengths in OPT3 which enable more base pairing interactions, thereby forming more stable structures that are less prone to dissociation (Kammer et al., 2020). However, despite OPT2 having the longest stem length like OPT3, it exhibited the lowest folding stability, likely due to the presence of bulge loop that disrupted continuation of the first stem. The structural destabilizing effect of bulge loop can significantly reduce the stability of aptamer structures as it interrupts regular base pairing in stems (Crowther et al., 2017). Although OPT1 has the shortest stem length, it exhibits higher folding stability than OPT2. This suggests that factors beyond stem length and loop type influence overall stability. Notably, OPT1 has the highest GC content in its stem regions (80%) compared to OPT2 (66.67%) and OPT3 (58%), supporting that higher GC content enhances stability through increased melting temperature. Additionally, OPT3 demonstrated an optimal length of 38 nucleotides, falling within the typical range of 25 to 40 nucleotides required for effective target interaction, and incorporates key structural motifs such as stem-loops and G-quadruplexes (Koshmanova et al., 2024). These findings suggest that OPT3 offers the most promising design, combining stable folding with an optimal aptamer length.

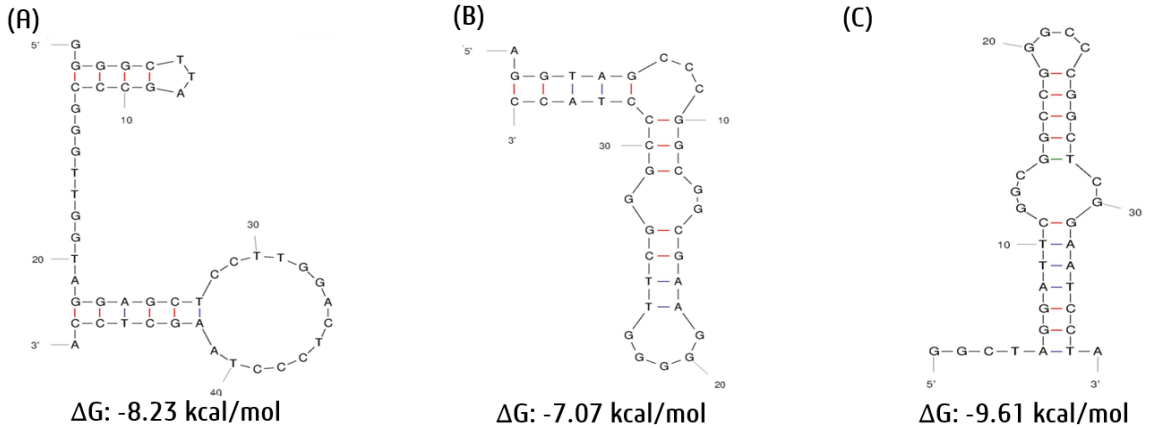

Figure 3 2D structures and folding stability values (ΔG) of optimized aptamers: (A) OPT1, (B) OPT2, and (C) OPT3.

The optimized aptamers were re-docked at the dimer interface of G6PD^{Nashville} and G6PD^{Canton}, and their docking results were visualized using PyMOL to evaluate their binding poses. AG1 was superimposed with each aptamer's binding pose to help localize the dimer interface. As depicted in Figure 4, OPT3 exhibited the most favourable binding pose, structurally coinciding with AG1's binding

region. In contrast, OPT1 and OPT2 showed only partial overlap with AG1. These findings highlight OPT3 as the most promising candidate, followed by OPT2 and OPT1, effectively mimicking AG1's binding mode by closely aligning with its position at the dimer interface.

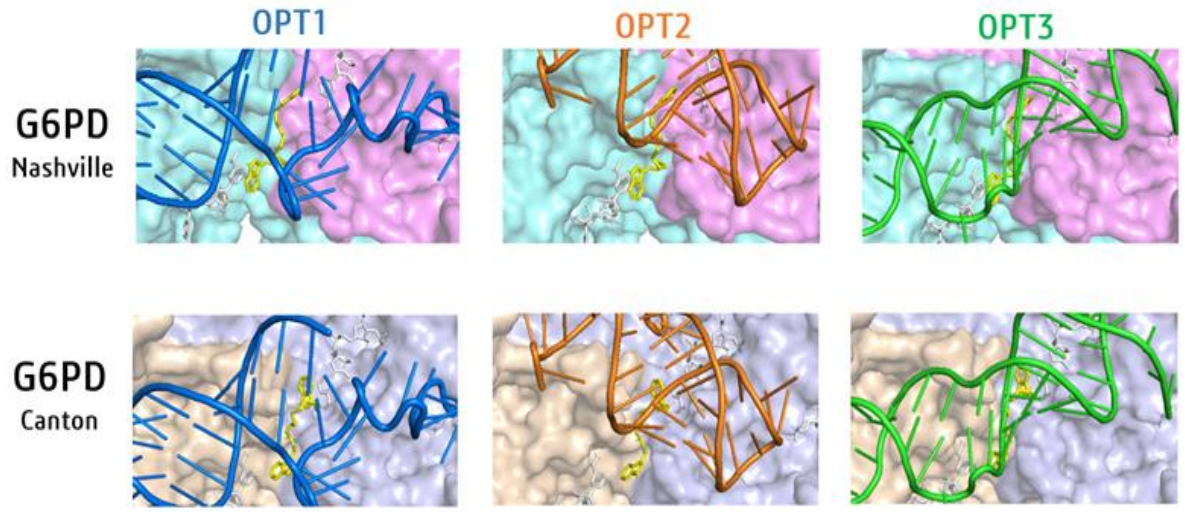

Figure 4 Superimpose of AG1 (yellow stick) and three optimized aptamers (OPT1: blue; OPT2: orange, OPT3: green) at the enzyme dimer interface.

Compared to AG1 as the reference compound, the optimized aptamers exhibited significantly higher binding affinities at the dimer interface of both G6PD^{Nashville} and G6PD^{Canton}, as shown in Table 2. The more negative binding energy (ΔG) values indicate that the aptamer–protein binding was more energetically favourable than those of AG1. This difference in binding affinity can be attributed to the fundamental structural differences between the small molecule and the aptamer in their binding and interaction with target proteins. Aptamers are single-stranded nucleic acids with a flexible phosphodiester backbone that allow them to fold into diverse secondary structures, such as stem-loops, hairpins, and G-quadruplexes (Shraim et al., 2022). These secondary structures further assemble into stable and unique three-dimensional structures through π–π stacking, hydrogen bonding between the bases, enabling them to bind to the target with high shape complementarity and specificity (Gelinas et al., 2016). In this study, the aptamers were designed and optimized to form structural motifs like stem-loop and G-quadruplex, which serve as scaffolds that arrange specific nucleotides for precise interactions with protein binding pockets (Zhang et al., 2021). These unique nucleic acid architectures allow aptamers to form stable and complementary interactions with their target proteins, contributing to their enhanced binding affinity and specificity compared to small molecules.

Table 2: Binding affinities of AG1 and optimized aptamers after docking to the dimer interface of G6PD^{Nashville} and G6PD^{Canton}.

Ligand	Binding Affinity, ΔG (kcal/mol)	
	G6PD^{Nashville}	G6PD^{Canton}
AG1	-6.8	-6.3
OPT1	-13.7	-14.7
OPT2	-18.1	-20.4
OPT3	-16.9	-18.8

OPT2, with the highest number of loops in its secondary structure compared to OPT1 and OPT3, demonstrated the strongest binding affinities, with the lowest binding energies of −19.1 kcal/mol and −20.4 kcal/mol against G6PDNashville and G6PDCanton, respectively. Aptamers possessing a greater number of loop regions generally exhibit enhanced binding affinity, as these loops often serve as primary interaction sites with the target protein (Debiais et al., 2020; Xu et al., 2023). Furthermore, the

GC content within loop regions also plays a significant role in modulating binding affinity. Higher GC content stabilizes the adjacent stem structures, thereby reinforcing the overall loop configuration and facilitating more effective target interaction (Lau et al., 2025). This observation may account for the comparatively higher binding affinity exhibited by OPT3, which possesses 100% GC content within its loop regions, in contrast to OPT1, which contains only 47.1% GC content despite both aptamers having the same number of loops.

The docking results were subsequently analyzed using BIOVIA Discovery Studio to visualize the 3D interactions between the aptamer and protein, including hydrogen bonds, salt bridges, and electrostatic interactions. In addition, LigPlot+ was used to generate 2D interaction diagrams, highlighting hydrophobic contacts and van der Waals forces. Understanding aptamer-protein interactions is crucial for elucidating the binding mechanism of aptamers in enzyme stabilization, as their binding is primarily governed by non-covalent intermolecular interactions, including hydrogen bonding, electrostatic forces, and van der Waals interactions (Zhang et al., 2023). Among the optimized aptamers, OPT3 exhibited the strongest binding interaction profile, characterized by the highest number of interactions, including hydrogen bonds, electrostatic forces, and hydrophobic contacts at the dimer interface of both $G6PD^{Nashville}$ and $G6PD^{Canton}$, as presented in Table 3. These non-covalent intermolecular interactions contribute to the overall stability of the enzyme (Adhav & Saikrishnan, 2023).

Table 3: Number of interactions formed by AG1 and aptamers after docking to the dimer interface of $G6PD^{Nashville}$ and $G6PD^{Canton}$.

Target Protein	Ligand	Number of interactions			
		Hydrogen Bond	Salt Bridge	Electrostatic	Hydrophobic
$G6PD^{Nashville}$	AG1	3	0	0	6
	OPT1	1	1	4	9
	OPT2	3	1	5	11
	OPT3	7	0	5	13
$G6PD^{Canton}$	AG1	2	0	0	6
	OPT1	2	1	4	9
	OPT2	6	3	5	11
	OPT3	8	0	5	12

Remarkably, residue ARG427 is particularly significant due to its role in salt bridge formation in the wild-type G6PD enzyme, a structural interaction lost in $G6PD^{Nashville}$ (Alakbaree et al., 2023). Among the three optimized aptamers, only OPT3 forms electrostatic contact with ARG427 in $G6PD^{Nashville}$, suggesting its potential to restore this lost interaction and enhance structural stability, as shown in Figure 5(A). Furthermore, $G6PD^{Canton}$ is known to exhibit a loss of inter-helical interactions, resulting in the displacement of α-helices and a significant reduction in both enzyme activity and structural stability (Hwang et al., 2020). Given that hydrogen bonds are crucial in stabilizing inter-helical interactions within α-helices, OPT3 may offer enhanced stabilization compared to AG1, OPT1 and OPT2, as supported by its formation of the highest number of hydrogen bonds, as illustrated in Figure 5(B).

Hence, these results clearly indicate that OPT3 is the most promising candidate among the aptamers, potentially offering stronger stabilization than AG1 as a G6PD activator due to its strongest binding profile. Although OPT2 also exhibited improved binding to $G6PD^{Canton}$, OPT3 remains the most favourable due to its consistent and robust performance across both G6PD mutants. This consistency suggests that OPT3 may also apply to other G6PD variants, with the potential to achieve better and more consistent binding performance across different mutants (Dong et al., 2021).

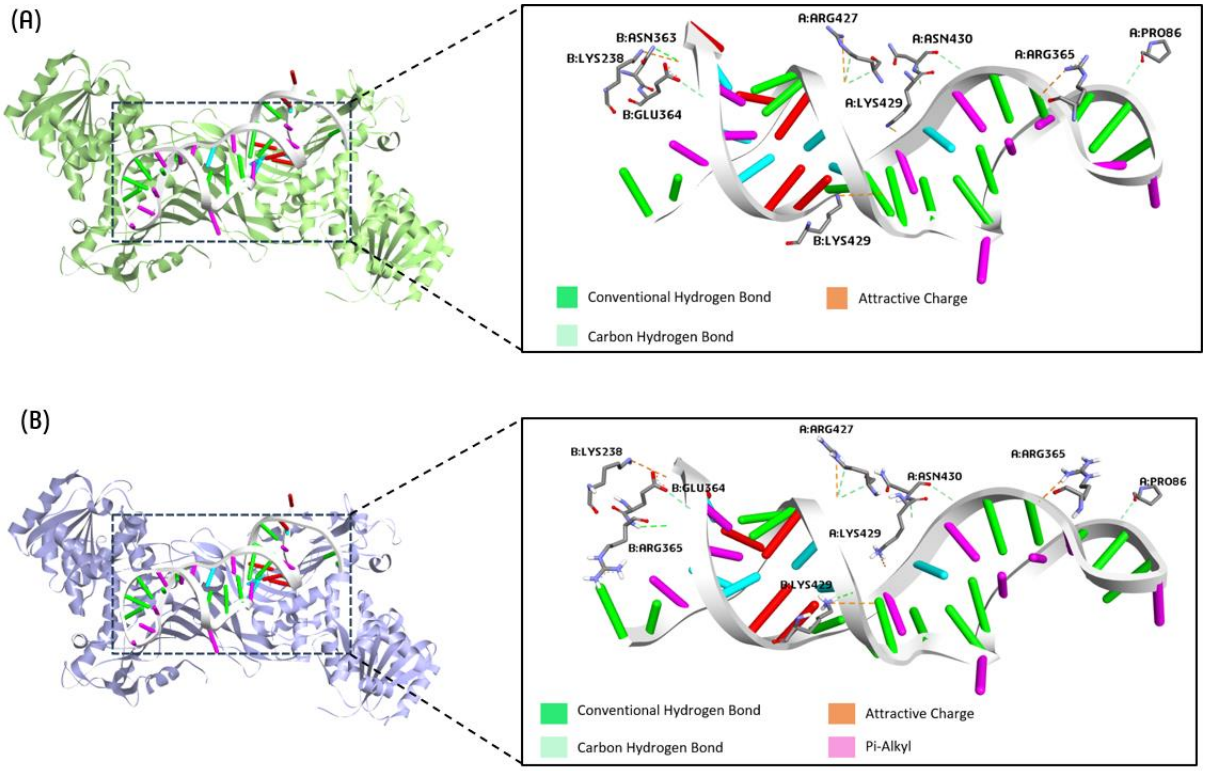

Figure 5 3D interaction mapping of OPT3 with (A) G6PD^{Nashville} and (B) G6PD^{Canton}, generated using BIOVIA Discovery Studio.

Conclusion

This study presents the first *in silico* design of G-quadruplex-forming DNA aptamers as potential G6PD activators targeting the dimer interface of two Class A mutants, G6PD^{Nashville} and G6PD^{Canton}, both associated with severe clinical phenotypes. The computational design and optimization approach adopted here offers a time-efficient, less labour-intensive, and cost-effective alternative to traditional SELEX methods. Through molecular docking analysis, the binding affinity, orientation, and interactions of three optimized aptamers were compared with those of AG1 to evaluate their activating potential against both G6PD^{Nashville} and G6PD^{Canton}. All aptamers exhibited higher binding affinities and stronger interfacial interactions than AG1, largely due to structural motifs, such as stem-loop formations, that promote high target affinity and stable interactions. Among the candidates, OPT3 emerged as the most promising G6PD activator, showing higher binding affinity toward the dimer interface of both G6PD mutants than AG1. Notably, OPT3 was the only aptamer whose binding pose overlapped with that of AG1 while demonstrating the strongest interaction profile, including a greater number of hydrogen bonds, electrostatic interactions, and hydrophobic contacts. These features suggest that OPT3 may offer superior stabilizing effects at the dimer interface. Overall, this study introduces the first aptamer specifically designed to target G6PD, highlighting its potential as a novel therapeutic strategy for restoring enzyme activity in G6PD deficiency.

Acknowledgement

This work was supported by the Undergraduate Research Opportunities Program (UROP) at UTM. Special thanks to Biogenes Technologies for their support and contribution to this study.

References

Adhav, V. A., & Saikrishnan, K. (2023). The realm of unconventional noncovalent interactions in proteins: Their significance in structure and function. *ACS Omega, 8*(25), 22731–22742.

Ahmad Najib, M., Winter, A., Mustaffa, K.M.F., Ong, E.B.B., Selvam, K., Khalid, M.F., Awang, M.S., Abd Manaf, A., Bustami, Y. and Aziah, I. (2024). Isolation and characterization of DNA aptamers against the HlyE antigen of *Salmonella Typhi*. *Scientific Reports, 14*(1), 28416.

Alakbaree, M., Abdulsalam, A. H., Ahmed, H. H., Ali, F. H., Al-Hili, A., Omar, M. S. S., Alonazi, M., Jamalis, J., Ab Latif, N., Hamza, M. A., & Amran, S. I. (2023). A computational study of structural analysis of Class I human glucose-6-phosphate dehydrogenase (G6PD) variants: Elaborating the correlation to chronic non-spherocytic hemolytic anemia (CNSHA). *Computational Biology and Chemistry, 104*, 107873.

Alakbaree, M., Amran, S., Shamsir, M., Ahmed, H. H., Hamza, M., Alonazi, M., Warsy, A., & Ab Latif, N. (2022). Human G6PD variant structural studies: Elucidating the molecular basis of human G6PD deficiency. *Gene Reports, 27*, 101634.

Bruno, J. G. (2022). Successes and failures of static aptamer-target 3D docking models. *International Journal of Molecular Sciences, 23*(22), 14410.

Crowther, C. V., Jones, L. E., Morelli, J. N., Mastrogiacomo, E. M., Porterfield, C., Kent, J. L., & Serra, M. J. (2017). Influence of two bulge loops on the stability of RNA duplexes. *RNA, 23*(2), 217–228.

Debiais, M., Lelievre, A., Smietana, M., & Müller, S. (2020). Splitting aptamers and nucleic acid enzymes for the development of advanced biosensors. *Nucleic Acids Research, 48*(7), 3400–3422.

Dong, L., Qu, X., Zhao, Y., & Wang, B. (2021). Prediction of binding free energy of protein–ligand complexes with a hybrid molecular mechanics/generalized born surface area and machine learning method. *ACS Omega, 6*(48), 32938–32947.

Gelinas, A. D., Davies, D. R., & Janjic, N. (2016). Embracing proteins: Structural themes in aptamer–protein complexes. *Current Opinion in Structural Biology, 36*, 122–132.

Gragoudas, E. S., Adamis, A. P., Cunningham, E. T., Feinsod, M., & Guyer, D. R., for the VEGF Inhibition Study in Ocular Neovascularization Clinical Trial Group. (2004). Pegaptanib for neovascular age-related macular degeneration. *The New England Journal of Medicine, 351*(27), 2805–2816.

Hui, Y., Yang, D., Wang, W., Liu, Y., He, C., & Wang, B. (2023). Truncated affinity-improved aptamer for selective and sensitive detection of streptomycin in dairy products with label-free electrochemical aptasensor. *Journal of Food Composition and Analysis, 121*, 105422.

Hwang, S., Mochly-Rosen, D., Chen, C. H., & Raub, A. G. (2020). *U.S. Patent Application No. 16/632,863*.

Hwang, S., Mruk, K., Rahighi, S., Raub, A. G., Chen, C. H., Dorn, L. E., Horikoshi, N., Wakatsuki, S., Chen, J. K., & Mochly-Rosen, D. (2018). Correcting glucose-6-phosphate dehydrogenase deficiency with a small-molecule activator. *Nature Communications, 9*(1), 4045.

Ji, D., Wang, B., Lo, K. W., Tsang, C. M., & Kwok, C. K. (2025). Pre-defined stem-loop structure library for the discovery of L-RNA aptamers that target RNA G-quadruplexes. *Angewandte Chemie International Edition, 64*(5), e202417247.

Kammer, M. N., Kussrow, A. K., Olmsted, I. R., Jackson, G. W., & Bornhop, D. J. (2020). Free solution assay signal modulation in variable-stem-length hairpin aptamers. *ACS Omega, 5*(20), 11308–11313.

Koshmanova, A.A., Artyushenko, P.V., Shchugoreva, I.A., Fedotovskaya, V.D., Luzan, N.A., Kolovskaya, O.S., Zamay, G.S., Lukyanenko, K.A., Veprintsev, D.V., Khilazheva, E.D. and Zamay, T.N. (2024). Aptamer's structure optimization for better diagnosis and treatment of glial tumors. *Cancers, 16*(23), 4111.

Lau, H. L., Zhao, H., Feng, H., & Kwok, C. K. (2025). Specific targeting and imaging of RNA G-quadruplex (rG4) structure using non-G4-containing L-RNA aptamer and fluorogenic L-aptamer. *Small Methods, 9*(3), 2401097.

Louis, N. E., Hamza, M. A., Baharuddin, P. N. E. B., Chandran, S., Latif, N. A., Alonazi, M. A., Halim, K. B. A., Warsy, A., & Amran, S. I. (2022). Preliminary study of structural changes of glucose-6-phosphate dehydrogenase deficiency variants. *BioMedicine, 12*(3), 12–19.

Nguyen, M. D., Osborne, M. T., Prevot, G. T., Churcher, Z. R., Johnson, P. E., Simine, L., & Dauphin-Ducharme, P. (2024). Truncations and in silico docking to enhance the analytical response of aptamer-based biosensors. *Biosensors and Bioelectronics, 265*, 116680.

O'Steen, M. R., & Kolpashchikov, D. M. (2022). A self-assembling split aptamer multiplex assay for SARS-COVID19 and miniaturization of a malachite green DNA-based aptamer. *Sensors and Actuators Reports, 4*, 100125.

Pakparnich, P., Sudsumrit, S., Imwong, M., Suteewong, T., Chamchoy, K., Pakotiprapha, D., Leartsakulpanich, U., & Boonyuen, U. (2021). Combined effects of double mutations on catalytic activity and structural stability contribute to clinical manifestations of glucose-6-phosphate dehydrogenase deficiency. *Scientific Reports, 11*(1), 24307.

Roxo, C., Kotkowiak, W., & Pasternak, A. (2019). G-quadruplex-forming aptamers—Characteristics, applications, and perspectives. *Molecules, 24*(20), 3781.

Shraim, A. A. S., Abdel Majeed, B. A., Al-Binni, M. A., & Hunaiti, A. (2022). Therapeutic potential of aptamer–protein interactions. *ACS Pharmacology & Translational Science, 5*(12), 1211–1227.

Soon, S., & Nordin, N. A. (2019). In silico predictions and optimization of aptamers against *Streptococcus agalactiae* surface protein using computational docking. *Materials Today: Proceedings, 16*, 2096–2100.

Soundararajan, S., Chen, W., Spicer, E. K., Courtenay-Luck, N., & Fernandes, D. J. (2008). The nucleolin-targeting aptamer AS1411 destabilizes Bcl-2 messenger RNA in human breast cancer cells. *Cancer Research, 68*(7), 2358–2365.

Tsukakoshi, K., Yamagishi, Y., Kanazashi, M., Nakama, K., Oshikawa, D., Savory, N., Matsugami, A., Hayashi, F., Lee, J., Saito, T., Sode, K., Khunathai, K., Kuno, H., & Ikebukuro, K. (2021). G-quadruplex-forming aptamer enhances the peroxidase activity of myoglobin against luminol. *Nucleic Acids Research, 49*(11), 6069–6081.

World Health Organization. (2022). *Technical consultation to review the classification of glucose-6-phosphate dehydrogenase (G6PD)*. Geneva: World Health Organization.

Xu, G., Wang, C., Yu, H., Li, Y., Zhao, Q., Zhou, X., Li, C. & Liu, M. (2023). Structural basis for high-affinity recognition of aflatoxin B1 by a DNA aptamer. *Nucleic Acids Research, 51*(14), 7666–7674.

Zhang, H. L., Lv, C., Li, Z. H., Jiang, S., Cai, D., Liu, S. S., & Zhang, K. H. (2023). Analysis of aptamer-target binding and molecular mechanisms by thermofluorimetric analysis and molecular dynamics simulation. *Frontiers in Chemistry, 11*, 1144347.

Zhang, N., Chen, Z., Liu, D., Jiang, H., Zhang, Z.-K., Lu, A., Zhang, B.-T., Yu, Y., & Zhang, G. (2021). Structural biology for the molecular insight between aptamers and target proteins. *International Journal of Molecular Sciences, 22*(8), 4093.